Cation Distribution in $(M', M)_3Se_4$

II. $(V, Ti)_3Se_4$ and $(Cr, V)_3Se_4$

A. HAYASHI, Y. UEDA, AND K. KOSUGE

*Department of Chemistry, Faculty of Science,
Kyoto University, Kyoto, Japan*

H. MURATA AND H. ASANO

*Institute of Materials Science, University of Tsukuba, Sakura-mura,
Niihari-gun, Ibaraki, Japan*

N. WATANABE

*National Laboratory for High Energy Physics, Oho-machi, Tsukuba-gun,
Ibaraki, Japan*

AND F. IZUMI

*National Institute for Research in Inorganic Materials, Sakura-mura,
Niihari-gun, Ibaraki, Japan*

The cation distribution among the two crystallographic cation sites of the Cr_3S_4 structure was determined in VTi_2Se_4 and VCr_2Se_4 by high-resolution neutron diffraction, using Rietveld analysis. The results showed a considerable disorder but they nevertheless revealed the site preference of V atoms for the $2(a)$ site in both compounds. The compositional changes of the lattice parameters and the transition temperatures to the CdI_2-type structure in $(V_xTi_{1-x})_3Se_4$ and $(Cr_xV_{1-x})_3Se_4$ were compared with those in $(Cr_xTi_{1-x})_3Se_4$ and $(Fe_xCr_{1-x})_3Se_4$, and discussed from the viewpoint of the site preference of the cation. © 1987 Academic Press, Inc.

Introduction

Most of the $3d$-transition metal chalcogenides with chemical formula M_3X_4 (M: $3d$-transition metal, X: S, Se, Te) have the spinel structure or the Cr_3S_4 structure, as shown in Table I. The chalcogenide stacking is *ccp* for the spinel structure and *hcp* for the Cr_3S_4 structure. In both structures,

there are two crystallographic sites for metal ions and these compounds are expressed as $(M)[M_2]X_4$ based on the distinction of sites occupied by metal ions. In the expression $(M)[M_2]X_4$, ( ) and [ ] denote tetrahedral and octahedral voids in the spinel structure, respectively. In contrast, both ( ) and [ ] denote octahedral voids in the Cr_3S_4 structure. The characteristic of

237

the Cr_3S_4 structure is that it is vacancy-or-dered, which has been evidenced from the observation of the phase transition from the Cr_3S_4 to CdI_2 type at higher temperatures in several compounds (1–4). Like other com-pounds with similar vacancy-ordered struc-tures based on the CdI_2 structure, M_5X_8, M_2X_3, M_7X_8, etc., have also been found in several MX–MX_2 systems (5, 6). These structures are easily understood by follow-ing general principles. In the intermediate composition $M_{1+y}X_2$ ($0 < y < 1$) between MX with the NiAs structure and MX_2 with the CdI_2 structure, excess metal atoms of fraction y partially occur in the unoccupied layer (van der Waals' gap) in the CdI_2 struc-ture and are regularly arranged because of metal–vacancy or metal–metal interac-tions. The Cr_3S_4 structure appears at $y = 0.5$, and the layer stacking in this structure is expressed as $M^FXM^VXM^FX \ldots$, where M^F denotes the metal layer fully oc-cupied ($4(i)$ sites) and M^V the half-filled and ordered metal layer ($2(a)$ sites) (see Fig. 1). The unit cell is described in terms of the basic CdI_2 structure as $a_m \approx \sqrt{3}a_h$, $b_m \approx a_h$, and $c_m \approx 2c_h$, where a_m, b_m, and c_m are the lattice parameters of the Cr_3S_4 structure having the monoclinic space group $I2/m$; a_h and c_h are lattice parameters of the hexago-nal CdI_2 structure.
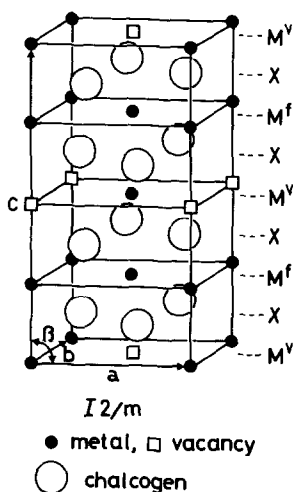
From the structural aspect, many mixed-metal compounds $M'M_2X_4$ with the Cr_3S_4 structure have also been synthesized and their physical properties have been studied. Chevreton and Andron (7) proposed such metal-ordered structures as normal-type $(M')[M_2]X_4$ and inverse-type $(M)[M'M]X_4$ on these compounds from analogy of spinel compound, where ( ) denotes the half-filled metal layer M^V and [ ] the filled metal layer M^F. In fact, such a metal-or-dered structure has been confirmed in sev-eral compounds mainly by neutron diffrac-tion or Mössbauer spectroscopy (7–13). To understand the physical properties and chemical bonds of these compounds, it is important to know the metal-ordered struc-ture or site preference. In the phase dia-gram of the ternary M'–M–X system, the compound $M'M_2X_4$ appears at the compo-sition $x = \frac{1}{3}$ in the pseudobinary system $(M'_x M_{1-x})_3X_4$ or $x = \frac{1}{2}$ in the system M'_xMX_2 ($0 < x < 1$). The site preference in $M'M_2X_4$ may be kept also in the pseudobinary sys-tems M'_3X_4–M_3X_4 or M'_xMX_2. We have also systematically studied the phase diagram and physical properties of the selenide sys-tem $(M'_xM_{1-x})_3Se_4$, because most of $3d$-transition metal selenides M_3Se_4 crystallize in the Cr_3S_4 structure (see Table I). In a previous paper (14), it was suggested that the compositional dependence of lattice pa-rameters in $(Cr_xTi_{1-x})_3X_4$ (X: Se, Te) gives us information about the metal-ordered structure of $CrTi_2Se_4$, $TiCr_2Se_4$, $CrTi_2Te_4$, and $TiCr_2Te_4$. In a succeeding paper (15), the cation distribution in $CrTi_2Se_4$ and $TiCr_2 Se_4$ was reported from Rietveld analysis of

TABLE I

CRYSTAL STRUCTURE OF M_3X_4 COMPOUNDS

| X | M | | | | | | |
	Ti	V	Cr	Mn	Fe	Co	Ni
S	—	Cr_3S_4	Cr_3S_4	—	Spinel	Spinel	Spinel
Se	Cr_3S_4	Cr_3S_4	Cr_3S_4	—	Cr_3S_4	Cr_3S_4	Cr_3S_4
Te	Cr_3S_4	Cr_3S_4	Cr_3S_4	—	Cr_3S_4	CdI_2	CdI_2

$I2/m$

● metal, □ vacancy

◯ chalcogen

FIG. 1. Cr_3S_4 structure ($I2/m$).

high-resolution neutron diffraction patterns, and the compositional dependence of magnetic properties in $(Cr_xTi_{1-x})_3Se_4$ was explained on the basis of the site preference of Cr ions for M^V layers. We proposed the existence of the compounds $(Co)[Ti_2]Se_4$, $(Ni)[Ti_2]Se_4$, and $(Ni)[V_2]Se_4$ from a recent study of their phase diagrams (16).

In this paper, we report the cation distribution in VTi_2Se_4 and VCr_2Se_4, determined from Rietveld analysis of high-resolution powder neutron diffraction patterns, together with the phase diagrams of $(V_xTi_{1-x})_3$ Se_4 and $(Cr_xV_{1-x})_3Se_4$ systems.

Experimental

Sample preparation was reported elsewhere (14). Phase characterizations were made at room temperature by powder X-ray diffraction with monochromatic $CuK\alpha$ radiation. Phase transitions at higher temperatures were detected by high-temperature X-ray diffraction *in situ* and differential thermal analysis (DTA). In order to

prevent oxidation or decomposition, samples were sealed in an evacuated silica capillary during the high-temperature X-ray diffraction measurement and in a cylindrical silica capsule during the DTA measurement. The neutron diffraction experiment was carried out with a high-resolution powder diffractometer HRP (17) at the KENS pulsed spallation neutron source in the National Laboratory for High Energy Physics. The experimental details have been reported in our previous paper (15).

Results and Discussion

Both $(V_xTi_{1-x})_3Se_4$ and $(Cr_xV_{1-x})_3Se_4$ systems exhibited a solid solution with the Cr_3S_4 structure over a whole composition range. Figures 2a and 2b show lattice parameters ($I2/m$: a, b, c, β) vs composition curves for both systems, determined by the least-squares method using more than 10 X-ray diffraction peaks. DTA and high-temperature X-ray measurements revealed that all the samples show a phase transition
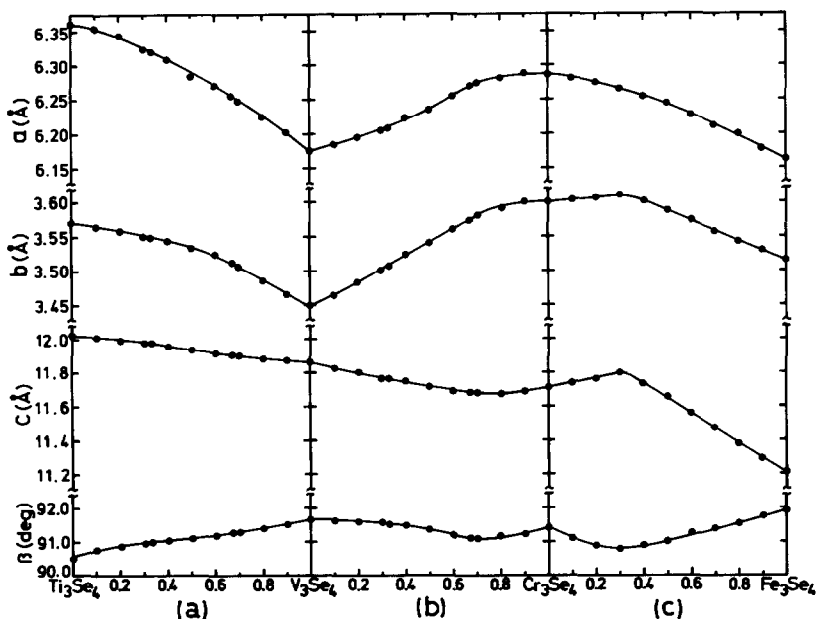

FIG. 2. Lattice parameters vs composition curves. (a) $(V_xTi_{1-x})_3Se_4$; (b) $(Cr_xV_{1-x})_3Se_4$; and (c) $(Fe_xCr_{1-x})_3Se_4$.

from the Cr_3S_4 (monoclinic) to CdI_2 (hexagonal) type accompanied by the disordering of vacancies. The hysteresis of the transition on heating and cooling was about 10°C for all samples. Phase diagrams obtained for both systems are shown in Figs. 3a and 3b.

VTi_2Se_4 and VCr_2Se_4 were studied by neutron diffraction. The diffraction data were analyzed by the Rietveld method (*18*). Figures 4a and 4b show the observed and calculated profiles of the two compounds VTi_2Se_4 and VCr_2Se_4, respectively. The final crystallographic parameters are given in Table II. The resulting cation distributions on two sites, M^V and M^F, are $(V_{0.60}Ti_{0.40})$ $[V_{0.40}Ti_{1.60}]Se_4$ for VTi_2Se_4 and $(V_{0.55}Cr_{0.45})$ $[V_{0.45}Cr_{1.55}]Se_4$ for VCr_2Se_4. The results reveal that V atoms have a tendency to prefer the M^V layer in both VTi_2Se_4 and VCr_2Se_4, although the cation distribution in both compounds is relatively disordered compared to the ideal one.

In selenides, it was determined by neutron diffraction that $CrTi_2Se_4$ (*15*) and Fe Cr_2Se_4 (*11*) are normal-type compounds and that $TiCr_2Se_4$ (*10, 14*) is inverse type; that is, Cr ions in $CrTi_2Se_4$ and $TiCr_2Se_4$,

TABLE II

FINAL ATOMIC PARAMETERS[a] FOR VTi_2Se_4 AND VCr_2Se_4 WITH ESTIMATED STANDARD DEVIATIONS IN PARENTHESES

Atom	Position	x	y	z	Occupancy
		VTi_2Se_4			
V(1)	2(a)	0	0	0	0.60(2)
Ti(1)	2(a)	0	0	0	0.40(2)
V(2)	4(i)	0.2547(8)	0.226(2)	0	0.20(2)
Ti(2)	4(i)	0.2547(8)	0.226(2)	0	0.80(2)
Se(1)	4(i)	0.6304(3)	0.2976(6)	0	1.0
Se(2)	4(i)	0.8861(3)	0.2235(6)	0	1.0

$a' = 13.6153$ Å; $b' = 6.2962$ Å; $c' = 3.5562$ Å; $\gamma = 118.42°$
$B^b = 0.19(2)$ Å^2; $R_{wp}{}^c = 5.15\%$; $R_B{}^d = 3.04\%$

		VCr_2Se_4			
V(1)	2(a)	0	0	0	0.55(1)
Cr(1)	2(a)	0	0	0	0.45(1)
V(2)	4(i)	0.2586(8)	0.238(2)	0	0.22(1)
Cr(2)	4(i)	0.2586(8)	0.238(2)	0	0.78(1)
Se(1)	4(i)	0.6338(3)	0.2974(7)	0	1.0
Se(2)	4(i)	0.8832(3)	0.2197(7)	0	1.0

$a' = 13.4049$ Å; $b' = 6.2801$ Å; $c' = 3.5784$ Å; $\gamma = 119.21°$
$B^b = 0.11(3)$ Å^2; $R_{wp}{}^c = 8.11\%$; $R_B{}^d = 4.30\%$

[a] In Rietveld analysis the reduced unit cell with space group $B2/m$ was adopted. The relation between lattice parameters described in space group $B2/m$ and $I2/m$ is as follows: $a = b'$, $b = c'$, $c = (a'^2 + b'^2 + 2a'b' \cos \gamma)^{1/2}$ and $\beta = \cos^{-1}[(a' \cos \gamma + b')/c'^{1/2}]$.
[b] B = overall thermal parameter.
[c] $R_{wp} = [\Sigma_i w_i\{Y_i(obs) - Y_i(cal)\}^2/\Sigma_i w_i\{Y_i(obs)\}^2]^{1/2}$. ($Y_i(obs)$ and $Y_i(cal)$ are observed and calculated counts for the ith channel and w_i is a weighting factor.)
[d] $R_B = \Sigma_k |I_k(obs) - I_k(cal)|/\Sigma_k I_k(obs)$. $I_k(obs)$ and $I_k(cal)$ are observed and calculated integrated intensities for the kth reflection.

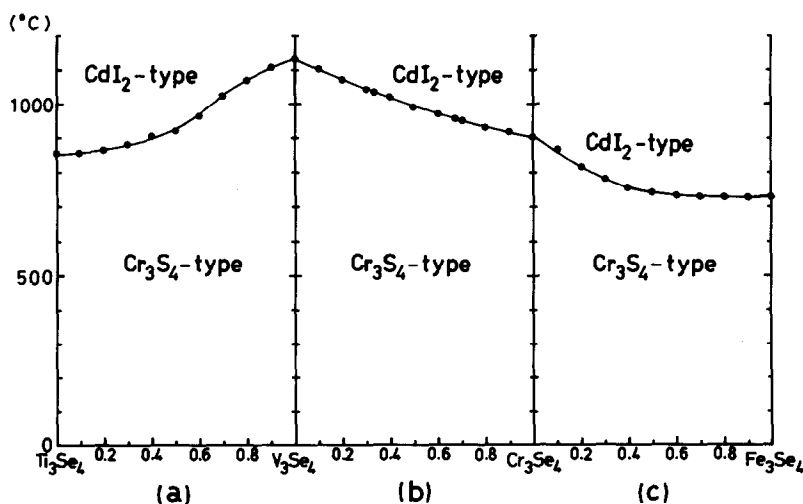FIG. 3. Phase diagrams. (a) $(V_xTi_{1-x})_3Se_4$; (b) $(Cr_xV_{1-x})_3Se_4$; and (c) $(Fe_xCr_{1-x})_3Se_4$.
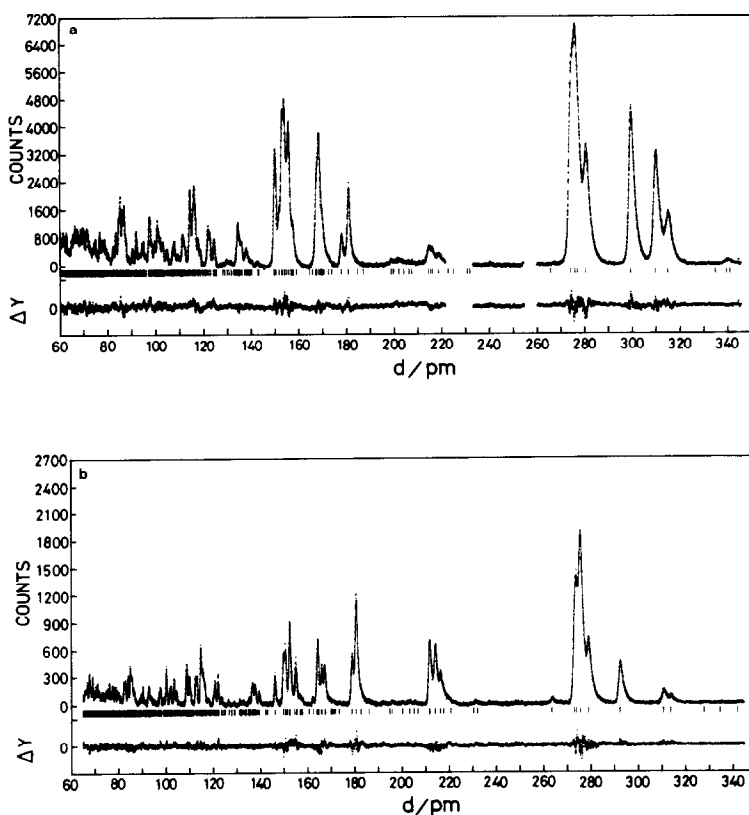
FIG. 4. Observed (dots) and calculated (solid lines) neutron diffraction patterns. (a) VTi_2Se_4 and (b) VCr_2Se_4. ΔY shows the difference between observed and calculated counts. The vertical markers indicate Bragg positions. Diffraction data at around $d = 225$ and 258 pm in (a) were omitted from the pattern because very weak peaks probably because of impurities appeared in these regions.

and Fe ions in $FeCr_2Se_4$ preferentially occupy the M^V layer.

Now let us discuss the site preference or metal-ordered structure in $(Cr_xV_{1-x})_3Se_4$ and $(V_xTi_{1-x})_3Se_4$ from Δc and ΔT_c (defined below), in comparison with $(Cr_xTi_{1-x})_3Se_4$ and $(Fe_xCr_{1-x})_3Se_4$. The compositional dependence of the lattice parameters and the phase diagram for $(Fe_xCr_{1-x})_3Se_4$ (19) are shown in Figs. 2c and 3c for reference. If the site preference is retained over the whole range of composition in the pseudo-binary solid solution $(M'_xM_{1-x})_3X_4$ system and M' prefers to occupy the M^V layer, the substitution in the ideal case should progress as follows:

$$0 \leqq x \leqq \tfrac{1}{3} \qquad (M'_{3x}M_{1-3x})[M_2]X_4$$

$$\tfrac{1}{3} \leqq x \leqq 1 \qquad (M')[M'_{3x-1}M_{3-3x}]X_4$$

with a turning point at $x = \tfrac{1}{3}(M'M_2X_4)$. As a measure of the site preference of metal ions, the compositional dependence of Δc^1 = [(observed c-axis) − (Vegard's law)] is shown in Fig. 5 for $(V_xTi_{1-x})_3Se_4$ and $(V_x Cr_{1-x})_3Se_4$, together with $(Cr_xTi_{1-x})_3Se_4$ and $(Fe_xCr_{1-x})_3Se_4$. In $(Cr_xTi_{1-x})_3Se_4$ and $(Fe_x$

[1] The c parameter was adopted to discuss the deviation from the Vegard's law because it can be more precisely determined compared to the other lattice parameters using high angle $(00l)$ diffraction with stronger intensity and because it is more sensitive to changes in composition.
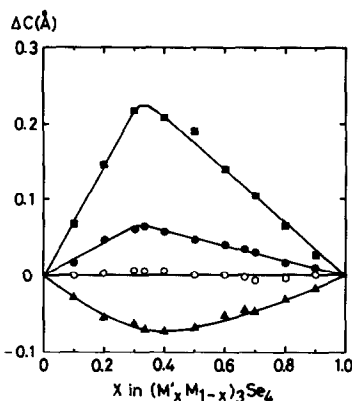
FIG. 5. Δc (see the text) vs composition curves of $(M'_xM_{1-x})_3Se_4$. O, $(V_xTi_{1-x})_3Se_4$; ▲, $(V_xCr_{1-x})_3Se_4$; ●, $(Cr_xTi_{1-x})_3Se_4$; ■, $(Fe_xCr_{1-x})_3Se_4$.

$Cr_{1-x})_3Se_4$, Δc shows a linear change in the composition range for both $0 < x < \frac{1}{3}$ and $\frac{1}{3} < x < 1$, as just obeying the Vegard's law between the intermediate compound $CrTi_2Se_4$ or $FeCr_2Se_4$ and the end members in each system. On the other hand, $\Delta c \approx 0$ over the whole composition range in $(V_xTi_{1-x})_3Se_4$ and there is a gradual change with a minimum around $x = 0.4$ in $(V_xCr_{1-x})_3Se_4$. These observations suggest that substitution in both systems does not progress with so clear a site preference as in the other two systems. This is consistent with the results that the cation distribution observed in VTi_2Se_4 and VCr_2Se_4 is rather random.

In addition to the vacancy disordering, disordering of metal arrangement among the M^V and M^F layers can also be expected at a critical temperature T_t; the degree of order naturally decreases with increasing temperature. The observed cation distribution corresponds to the degree of order at the temperature where the sample was annealed or at the lowest temperature where the diffusion of metal ions was possible. In DTA measurements, no anomaly corresponding to this transition was observed up to 1100°C in all samples. This means that the transition is of second order or T_t is

above 1100°C. The latter case is ruled out at least in VTi_2Se_4 and VCr_2Se_4, as judged by the results that the observed cation distribution of the samples prepared at temperature as low as 300°C is rather random.

Figure 6 shows the deviation ΔT defined as follows:

$$\Delta T = T_c - [(1 - x)T_{c1} + xT_{c2}],$$

where x is the composition in $(M'_xM_{1-x})_3X_4$ system, T_c is the transition temperature from the Cr_3S_4 to CdI_2 type and T_{c1} and T_{c2} are T_c for $x = 0$ (M_3X_4) and $x = 1$ (M'_3X_4), respectively. The curves show a minimum around $x = \frac{1}{3}$ in $(Cr_xTi_{1-x})_3Se_4$ and $(Fe_x Cr_{1-x})_3Se_4$ systems and around central composition $(x = \frac{1}{2})$ in $(V_xTi_{1-x})_3Se_4$ and $(V_x Cr_{1-x})_3Se_4$ systems. It is general in the solid solution system that ΔT changes smoothly with a minimum or maximum around central composition in the case that no intermediate compound exists. If a compound exists at an intermediate composition, ΔT changes in the same way between the intermediate compound and the end members. $(Cr_xTi_{1-x})_3Se_4$ and $(Fe_xCr_{1-x})_3Se_4$ systems seem to belong to the latter, having $CrTi_2Se_4$ and $FeCr_2Se_4$ with the metal-ordered structure as an intermediate compound. The former may be the case for $(V_xTi_{1-x})_3$
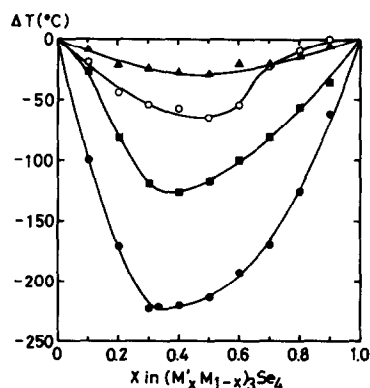

FIG. 6. ΔT (see the text) vs composition curves of $(M'_xM_{1-x})_3Se_4$. O, $(V_xTi_{1-x})_3Se_4$; ▲, $(V_xCr_{1-x})_3Se_4$; ●, $(Cr_xTi_{1-x})_3Se_4$; □, $(Fe_xCr_{1-x})_3Se_4$.

Se_4 and $(Cr_xV_{1-x})_3Se_4$. Therefore, T_t is likely to be higher than T_c in $(Cr_xTi_{1-x})_3Se_4$ and $(Fe_xCr_{1-x})_3Se_4$, and lower in $(V_xTi_{1-x})_3$ Se_4 and $(Cr_xV_{1-x})_3Se_4$. This is consistent with the results that cation distributions in VTi_2Se_4 and VCr_2Se_4 are more disordered than in $CrTi_2Se_4$ and $TiCr_2Se_4$ at the same annealing temperature of 300°C.

In conclusion, the cation distributions in VTi_2Se_4 and VCr_2Se_4 show considerable disorder but they nevertheless reveal the preference of V atoms for the M^V layer $(2(a)$ sites). Further, Fe ions selectively occupy the M^V layer in $(Fe_xCr_{1-x})_3Se_4$.

We have, at present, no explanation of the origin of such site preference; a key may be obtained when the site preference on all compounds with the Cr_3S_4 structure and the physical properties of those compounds are made clear.

A neutron diffraction study at various temperatures to confirm the transition to the metal-disordered state, as well as a Mössbauer study of the compounds containing Fe as a constituent element to determine the cation distribution or the site preference, is now in progress.

References

1. Y. OKA, K. KOSUGE, AND S. KACHI, *J. Solid State Chem.* **23**, 11 (1978).

2. H. WADA, *Bull. Chem. Soc. Japan* **52**, 2918 (1979).

3. T. OHTANI, R. FUJIMOTO, H. YOSHINAGA, M. NAKAHIRA, AND Y. UEDA, *J. Solid State Chem.* **48**, 161 (1983).

4. T. OHTANI, S. ONOUE, AND M. NAKAHIRA, *Mater. Res. Bull.* **19**, 1367 (1984).

5. F. JELLINEK, *Acta Crystallogr.* **10**, 620 (1957).

6. M. CHEVRETON, *Bull. Soc. Fr. Minéral. Cristallogr.* **90**, 592 (1967).

7. M. CHEVRETON AND B. ANDRON, *C.R. Acad. Sci. Ser. B* **264**, 316 (1967).

8. B. ANDRON, G. BÉRODIAS, M. CHEVRETON, AND P. MOLLARD, *C.R. Acad. Sci. Ser. B* **263**, 621 (1966).

9. B. ANDRON AND E. F. BERTAUT, *J. Phys. (Paris)* **27**, 619 (1966).

10. B. LAMBERT-ANDRON, G. BÉRODIAS, AND M. CHEVRETON, *Bull. Soc. Fr. Miner. Cristallogr.* **91**, 88 (1968).

11. K. ADACHI, K. SATO, AND K. KOJIMA, *Mem. Fac. Eng. Nagoya Univ.* **22**, 253 (1970).

12. I. KAWADA AND H. WADA, *Physica B* **105**, 223 (1981).

13. H. NOZAKI, H. WADA, AND H. YAMAMURA, *Solid State Commun.* **44**, 63 (1982).

14. Y. UEDA, K. KOSUGE, M. URABAYASHI, A. HAYASHI, S. KACHI, AND S. KAWANO, *J. Solid State Chem.* **56**, 263 (1985).

15. A. HAYASHI, Y. UEDA, K. KOSUGE, H. MURATA, H. ASANO, N. WATANABE, AND F. IZUMI, *J. Solid State Chem.* **67**, 346 (1987).

16. A. HAYASHI, K. IMADA, K. INOUE, Y. UEDA, AND K. KOSUGE, *Bull. Inst. Chem. Res. Kyoto Univ.* **64**, 186 (1986).

17. N. WATANABE, H. ASANO, H. IWASA, S. SATO, H. MURATA, T. FUKIURA, S. TOMIYOSHI, F. IZUMI, AND K. INOUE, "KENS Report-V, KEK Progress Report," 84-2, p. 581 (1982).

18. F. IZUMI, *J. Crystallogr. Soc. Japan* **27**, 23 (1985) [in Japanese].

19. In preparation.